



Journal of Applied Sciences

ISSN 1812-5654

science
alert

ANSI*net*
an open access publisher
<http://ansinet.com>

A State Observer and a Synchronization Method for Heart Pacemakers

¹H. Gholizade-Narm, ²A. Azemi, ¹M. Khademi and ³M. Karimi-Ghartemani

¹Faculty of Engineering, Ferdowsi University of Mashhad, Iran

²College of Engineering, Penn State University, USA

³Faculty of Electrical Engineering, Sharif University of Technology, Tehran, Iran

Abstract: In this study a synchronization method is developed to prevent the blocking arrhythmias which are caused by lack of synchronization between the two major heart pacemakers called the Sino-Atrial (SA) node and Atrio-Ventricular (AV) node. Such pacemakers can be modeled by the Van der Pol oscillators. Feedback linearization method is used in synchronization. Since all states are not always available, they are estimated by a new observer in this research. To design the observer, first we introduce a robust observer for a unique Van der Pol oscillator. The robustness of proposed observer is obtained using gain and phase margins test. The observer variables are such that the error dynamical system is linear time varying and we use describing function method to prove its convergence. This observer is then extended to two unidirectional and bidirectional coupled Van der Pol Oscillators. To prove the stability, a novel nonlinear function structure is introduced to seclude the coupled Van der Pol oscillators to two isolated oscillators. The performance of the proposed method is investigated by numerical simulations.

Key words: Coupled oscillators, state observer, cardiac pacemaker, synchronization, describing function, stability analysis

INTRODUCTION

The Van der Pol oscillator was introduced in 1927 by Van der Pol and Van der Mark (van der Pol and van der Mark, 1927). They succeeded to model heartbeat by this oscillator. The modeling of cardiac pacemakers also has been done with a little changes in the Van der Pol oscillator (Grudzinsky and Zebrowski, 2004; Sato *et al.*, 1994; Brando *et al.*, 1998). This oscillator has had many other applications in physics and biological science. For instance, Fitzhugh (1961) and Nagumo *et al.* (1962) extended it and introduced a model of neuron potential in biology.

Cardiac pacemakers modeling is one of the applications of Van der Pol oscillator. There are two major coupled pacemakers in cardia that generate and transfer the impulses which are needed for beating. The Sino-Atrial (SA) node is impulse generator and the Atrio-Ventricular (AV) node is a follower pacemaker that transfers impulses to ventricle. In the absence of SA node impulses, the AV node initiates impulse generation. In the normal mode, all impulses are generated in SA node and transferred to ventricle with a small delay via AV node. When the coupling intensity decreases, some impulses do not reach the ventricle and different types of blocking arrhythmias occur such as wenkebach, mobitz and others (Guyton and Hall, 2005). To prevent such arrhythmias, we propose a method to achieve synchronization.

Knowing all the state variables of the system is necessary in the synchronization method. Direct measurement of all states of system is impossible in practice, or it is too cost consuming to use or even the states might be virtual. Moreover, in some situations, the state estimation leads to better result in comparison with direct measurement because of measurement noise interferences. In linear systems, the Kalman filter has a good performance in the presence of noise for state estimation (Kalman, 1960). The Kalman filter was extended to nonlinear systems by Julier and Uhlmann (1997). In this method, first, the Jacobean matrix of system is calculated then the Kalman filter is used similar to linear system. Another method which has general usage is State Dependent Ricatti Equation method which introduced by Pearson (1962). Unfortunately, the two prior methods have stability issues.

There is not a general observer for nonlinear systems with guaranteed stability. Most of nonlinear observers are designed for a certain class of nonlinear systems or for a certain system. Hua *et al.* (2004) introduced an adaptive observer for a class of nonlinear systems. In that class, the system is divided into two parts: linear and nonlinear. The linear part must be Strictly Positive Real (SPR) and the nonlinear part must be globally Lipschitz. Many systems cannot satisfy these two conditions such as van

der Pol system. The major advantage of the Hua's method is its independence from Lipschitz constant which many observers depend on. Another observer is introduced for a class of nonlinear systems by Liao and Huang (1999) in which the nonlinear part should be globally Lipschitz and the linear part should be observable. Two major drawbacks of this method are its dependence on Lipschitz constant and the fact that the output must be a scalar. A sliding mode state and parameter estimator is presented by Floret-Ponet and Lamnabhi-Lagarigue (2001). For using this method, the nonlinear part must be Lipschitz and the system must be stable around the fixed point. The two aforementioned conditions are very restricting because most of the stable oscillators are unstable around the fixed point such as the van der Pol oscillator. The sliding mode is used in Zhang *et al.* (1999), too in which the system structure and parameters are unknown and only the output is known. It can estimate all states of the system but the major disadvantages are chattering problem and gain tuning which is difficult to achieve.

In this study, an observer is introduced for van der Pol oscillator and its convergence is proved. In addition, the gain and phase margins are obtained for a case study. The observer is extended to two van der Pol oscillators with unidirectional and bidirectional couplings and its convergence is proven in two ways. Finally, the introduced observer is used to design a synchronization strategy for two non-identical van der Pol oscillators and it is proven that the synchronization error tends to zero exponentially.

DESIGN OF OBSERVER

The procedure of designing the observer is divided in three parts. At first, an observer is designed for an insulated van der Pol oscillator. Then, it is extended to two unidirectional coupled oscillators. Finally, an observer is proposed for two bidirectional coupled oscillators.

Observer for an isolated van der pol: Consider the Van der Pol dynamical equation as:

$$\ddot{x} - \mu(1 - x^2)\dot{x} + \omega_1^2 x = 0 \tag{1}$$

where, μ and ω_1 are the nonlinear damping coefficient and intrinsic frequency in the lack of nonlinear term, respectively. Suppose the output is:

$$y = x \tag{2}$$

The dynamical systems (1) and (2) in the state space representation are:

$$\begin{aligned} \dot{x}_1 &= x_2 \\ \dot{x}_2 &= -\omega_1^2 x_1 + \mu_1(1 - x_1^2)x_2 \\ y = x_1 &= [1 \ 0]X, X = \begin{bmatrix} x_1 \\ x_2 \end{bmatrix} \end{aligned} \tag{3}$$

where, X is the state vector. The goal of this research is to design an observer that estimates all states of the system from the output.

The observer structure is proposed as:

$$\begin{aligned} \dot{\hat{x}}_1 &= \hat{x}_2 + f(x_1 - \hat{x}_1) \\ \dot{\hat{x}}_2 &= -\omega_1^2 \hat{x}_1 + \mu_1(1 - \hat{x}_1^2)\hat{x}_2 + g(x_1 - \hat{x}_1) \end{aligned} \tag{4}$$

where, $\hat{x} = [\hat{x}_1 \ \hat{x}_2]^T$ is the observer state vector and f and g are appropriate functions. Note, in the observer equations, x_1 and \hat{x}_1 are arranged particularly to guarantee the stability. We prove the observer convergence in Theorem 1.

Theorem 1: There exist functions f and g such that the trajectories of the observer (4) track those of the oscillator (3).

Proof: Define the observer errors as:

$$e_1 = x_1 - \hat{x}_1, e_2 = x_2 - \hat{x}_2 \tag{5}$$

where, $E = [e_1, e_2]^T$ is the error state vector. The error dynamical equations are:

$$\begin{aligned} \dot{e}_1 &= e_2 - f(e_1) \\ \dot{e}_2 &= -\omega_1^2 e_1 + \mu_1(1 - x_1^2)e_2 - g(e_1) \end{aligned} \tag{6}$$

The f and g functions are proposed as:

$$\begin{aligned} f(e_1) &= (a + \mu_1)e_1, a > 0 \\ g(e_1) &= \mu_1(a + \mu_1)e_1 \end{aligned} \tag{7}$$

where, a is a positive scalar as observer gain. By substituting f and g in (6),

$$\begin{aligned} \dot{e}_1 &= e_2 - (a + \mu_1)e_1 \\ \dot{e}_2 &= -(\omega_1^2 + \mu_1(a + \mu_1))e_1 + \mu_1 e_2 - \mu_1 x_1^2(t)e_2 \end{aligned} \tag{8}$$

where, $x_1(t)$ is periodic and bounded. Equation set 8 represents a linear time varying system. The block diagram of (8) can be shown in Fig. 1 that the time varying and time invariant parts are secluded from each other. where transfer function G is:

$$G(p) = \frac{p + a + \mu}{p^2 + ap + \omega^2} \tag{9}$$

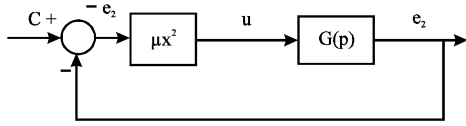


Fig. 1: Block diagram of observer error dynamical system

The approximate equivalent of time varying part is obtained using the Describing Function (DF) method (Slotine and Li, 1991). Suppose

$$x_1(t) = X \cos(\omega t + \varphi), \quad e_2 = E_2 \cos(\omega t) \quad (10)$$

The approximate equivalent is:

$$\begin{aligned} u(t) &= -\mu X^2 E_2 \cos(\omega t) \cos^2(\omega t + \varphi) \\ U_1 &= \frac{2}{\pi} \int_0^\pi (-\mu X^2 E_2 \cos^2 \theta \cos^2(\theta + \varphi)) d\theta \\ &= \frac{-\mu X^2 E_2}{4} (2 + \cos(2\varphi)) \\ N(X, \omega) &= \frac{\mu X^2}{4} (2 + \cos(2\varphi)) \end{aligned} \quad (11)$$

Figure 2 shows the typical Nyquist diagram of $G(j\omega)$ and

$$\frac{1}{N(X, \omega)}$$

According to the Nyquist criterion and Since $G(p)$ is stable, if the Nyquist diagram of $G(j\omega)$ intersects the point

$$\frac{1}{N(X, \omega)}$$

the system may have a limit cycle. If the diagram encircles the point, the system will be unstable. It can easily be seen that for all bounded X and φ in \mathfrak{R} space, the Nyquist diagram will be in the right hand of the critical point. Therefore, the error dynamical system is stable.

It can be interpreted from Fig. 2 that the gain margin is infinite. The phase margin is calculated as follows:

$$\begin{aligned} |G(j\omega^*)| &= \left| \frac{1}{N(X, \omega^*)} \right| \\ Pm &= \pi + \angle G(j\omega^*) \end{aligned} \quad (12)$$

Finding a closed form for the phase margin for all states is complicated. A numerical example is demonstrated in Fig. 3 in which the parameters are $\mu = 10$, $\omega_1 = 9$ and the phase-margin is plotted versus the observer gain a .

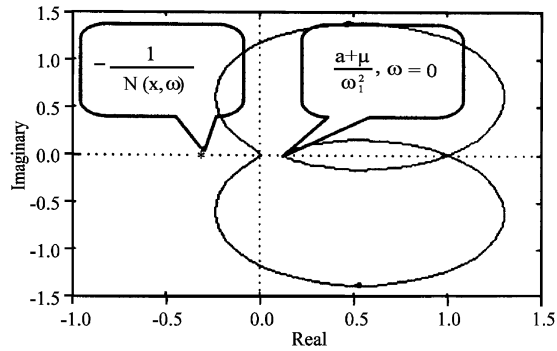


Fig. 2: Nyquist diagram of a typical transfer function

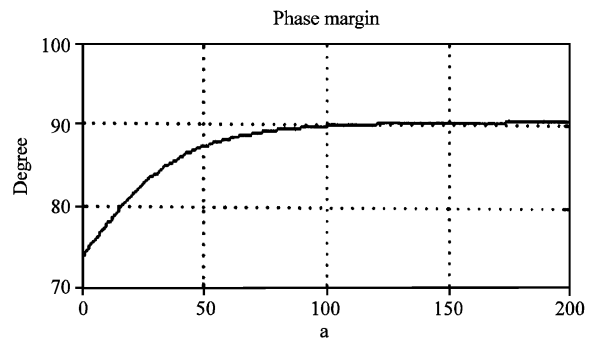


Fig. 3: Phase margin curve Vs. observer gain a

It can be shown from Fig. 3 that the minimum phase margin is 74° . The numerical simulation repeated for $0.1 < \mu < 15$, $1 < \omega_1 < 15$ (not shown here). The results show that the phase margin is always greater than 65.5° . According to gain margin and phase margin, it can be concluded that the observer is robust against disturbances.

Remark 1: The reason why the frequencies of x and e are equal is explained in Appendix A.

Remark 2: The parameter a controls the observer's convergence rate at the cost of noise sensitivity. A trade-off must be made when selecting its value.

Example 1 shows the observer performance for a unique Van der Pol system.

Observer for two unidirectional coupled van der Pol oscillators: The two unidirectional coupled van der Pol equations in state space representation are:

$$\begin{aligned} \dot{x}_1 &= x_2 \\ \dot{x}_2 &= -\omega_1^2 x_1 + \mu_1 (1 - x_1^2) x_2 \\ \dot{x}_3 &= x_4 \\ \dot{x}_4 &= -\omega_2^2 x_3 + \mu_2 (1 - x_3^2) x_4 + \alpha (x_1 - x_3) \\ y &= \begin{bmatrix} x_1 \\ x_3 \end{bmatrix} \end{aligned} \quad (13)$$

where, μ_1 and μ_2 are positive scalar damping coefficients, ω_1 and ω_2 are intrinsic frequencies of two oscillators and a is the positive coupling coefficient, $X = [x_1 \ x_2 \ x_3 \ x_4]^T$ is the system state vector and $y = [x_1 \ x_3]^T$ is the output vector. The observer system is proposed as follows:

$$\begin{aligned} \dot{\hat{x}}_1 &= \hat{x}_2 + f_1(x_1 - \hat{x}_1) \\ \dot{\hat{x}}_2 &= -\omega_1^2 \hat{x}_1 + \mu_1(1 - x_1^2)\hat{x}_2 + g_1(x_1 - \hat{x}_1) \\ \dot{\hat{x}}_3 &= \hat{x}_4 + f_2(x_3 - \hat{x}_3) \\ \dot{\hat{x}}_4 &= -\omega_2^2 \hat{x}_3 + \mu_2(1 - x_3^2)\hat{x}_4 + \alpha(\hat{x}_1 - \hat{x}_3) + g_2(x_3 - \hat{x}_3) \end{aligned} \tag{14}$$

where, $\hat{X} = [\hat{x}_1 \ \hat{x}_2 \ \hat{x}_3 \ \hat{x}_4]^T$ is the observer state vector and $f_{1,2}$ and $g_{1,2}$ are appropriate functions. In Theorem 2, the convergence of observer (14) is proven.

Theorem 2: There exist $f_{1,2}$ and $g_{1,2}$ functions such that the error between trajectories of (13 and 14) tend to zero.

Proof: Define the observer errors as:

$$\begin{aligned} e_1 &= x_1 - \hat{x}_1, \ e_2 = x_2 - \hat{x}_2 \\ e_3 &= x_3 - \hat{x}_3, \ e_4 = x_4 - \hat{x}_4 \end{aligned} \tag{15}$$

The error dynamical equations are:

$$\begin{aligned} \dot{e}_1 &= e_2 - f_1(e_1) \\ \dot{e}_2 &= -\omega_1^2 e_1 + \mu_1(1 - x_1^2)e_2 - g_1(e_1) \end{aligned} \tag{16}$$

$$\begin{aligned} \dot{e}_3 &= e_4 - f_2(e_3) \\ \dot{e}_4 &= -(\omega_2^2 + \alpha)e_3 + \mu_2(1 - x_3^2)e_4 - g_2(e_3) + \alpha e_1 \end{aligned} \tag{17}$$

Define $f_{1,2}$ and $g_{1,2}$ as follows:

$$\begin{aligned} f_1(e_1) &= (a_1 + \mu_1)e_1, \ a_1 > 0 \\ g_1(e_1) &= \mu_1(a_1 + \mu_1)e_1 \\ f_2(e_3) &= (a_2 + \mu_2)e_3, \ a_2 > 0 \\ g_2(e_3) &= \mu_2(a_2 + \mu_2)e_3 \end{aligned} \tag{18}$$

where, a_1 and a_2 are positive scalar values called observer gains. According to f_1 and g_1 definitions in (18) and substitution in (16) and using Theorem 1, e_1 and e_2 tend to zero based on Theorem 1. By substituting f_2 and g_2 in (17), the achieved equations are similar to (8) except αe_1 term which enters as a disturbance. Since this system is robust against disturbance as discussed earlier and because the disturbance tends to zero, therefore e_3 and e_4 tend to zero and (17) is stable.

Alternative proof: Define g_2 in (17) as follows:

$$g_2(e_1, e_3) = \mu_2(a_2 + \mu_2)e_3 + \alpha(e_3 - e_1), a_2 > 0 \tag{19}$$

By substituting g_2 in (17) and rewriting (16) and (17), the error dynamical system is:

$$\begin{aligned} \dot{e}_1 &= e_2 - (a_1 + \mu_1)e_1 \\ \dot{e}_2 &= -(\omega_1^2 + \mu_1(a_1 + \mu_1))e_1 + \mu_1 e_2 - \mu_1 x_1^2(t)e_2 \\ \dot{e}_3 &= e_4 - (a_2 + \mu_2)e_3 \\ \dot{e}_4 &= -(\omega_2^2 + \mu_2(a_2 + \mu_2))e_3 + \mu_2 e_4 - \mu_2 x_3^2(t)e_4 \end{aligned} \tag{20}$$

The Eq. 20 show that the system is composed of two isolated subsystems that are stable as discussed in Theorem 1. Therefore (20) is stable and the error tends to zero.

Example 2 shows the observer performance for two unidirectional-coupled Van der Pol systems.

Observer for two bidirectional coupled oscillators: The dynamical equations of bidirectional coupled oscillators in state space is:

$$\begin{aligned} \dot{x}_1 &= x_2 \\ \dot{x}_2 &= -\omega_1^2 x_1 + \mu_1(1 - x_1^2)x_2 + \alpha_1(x_3 - x_1) \\ \dot{x}_3 &= x_4 \\ \dot{x}_4 &= -\omega_2^2 x_3 + \mu_2(1 - x_3^2)x_4 + \alpha_2(x_1 - x_3) \\ y &= \begin{bmatrix} x_1 \\ x_3 \end{bmatrix} \end{aligned} \tag{21}$$

where, α_1 and α_2 are the positive scalar coupling coefficients. Define observer equations as follow:

$$\begin{aligned} \dot{\hat{x}}_1 &= \hat{x}_2 + f_1(x_1 - v_1) \\ \dot{\hat{x}}_2 &= -\omega_1^2 \hat{x}_1 + \mu_1(1 - x_1^2)\hat{x}_2 + \alpha_1(x_3 - x_1) \\ &\quad + g_1(x_1 - \hat{x}_1, x_3 - \hat{x}_3) \\ \dot{\hat{x}}_3 &= \hat{x}_4 + f_2(x_3 - \hat{x}_3) \\ \dot{\hat{x}}_4 &= -\omega_2^2 \hat{x}_3 + \mu_2(1 - x_3^2)\hat{x}_4 + \alpha_2(\hat{x}_1 - \hat{x}_3) \\ &\quad + g_2(x_1 - \hat{x}_1, x_3 - \hat{x}_3) \end{aligned} \tag{22}$$

Theorem 3: For the observer definition (22), there exist $f_{1,2}$ and $g_{1,2}$ functions such that the error variables (15) tend to zero.

Proof: The functions are proposed as:

$$\begin{aligned} g_1(e_1, e_3) &= \mu_1(a_1 + \mu_1)e_1 + \alpha_1(e_1 - e_3), a_1 > 0 \\ g_2(e_1, e_3) &= \mu_2(a_2 + \mu_2)e_3 + \alpha_2(e_3 - e_1), a_2 > 0 \end{aligned} \tag{23}$$

By substituting the functions in (22), the error dynamical equations are obtained as:

$$\begin{aligned} \dot{e}_1 &= e_2 - (a_1 + \mu_1)e_1 \\ \dot{e}_2 &= -(\omega_1^2 + \mu_1(a_1 + \mu_1))e_1 + \mu_1 e_2 - \mu_1 x_1^2(t)e_2 \\ \dot{e}_3 &= e_4 - (a_2 + \mu_2)e_3 \\ \dot{e}_4 &= -(\omega_2^2 + \mu_2(a_2 + \mu_2))e_3 + \mu_2 e_4 - \mu_2 x_3^2(t)e_4 \end{aligned} \tag{24}$$

By looking carefully to (24), it is concluded that the error dynamical system is composed of two isolated subsystem similar to (8) and it was proved in Theorem 1 that such subsystems are stable. Since these subsystems are isolated, therefore the whole system (24) is stable and error variables tend to zero.

Example 3 shown the observer performance for two bidirectional-coupled van der Pol systems.

Notice: An alternative proof for the stability of (24) is given in Appendix B.

DESIGN OF A SYNCHRONIZATION METHOD USING PROPOSED OBSERVER

As it is stated in Introduction, cardiac pacemakers modeling is one of the usages of van der Pol equation. In normal mode, the two major coupled pacemakers, SA and AV nodes are synchrony. When coupling intensity decreases, the AV node could not follow the SA node and various blocking arrhythmias arise such as Wenkebach, Mobitz and others. our goal is to synchronize two coupled pacemakers using feedback linearization method. It is assumed that only the SA and AV nodes action potential signals are available. Therefore the other states must be estimated by an observer. We use our proposed observer to do this task.

Since the effect of AV node on SA node is very little, it can be ignored in synchronization problem. Therefore the unidirectional coupling is considered. The equations are like (13) except:

$$\dot{x}_4 = -\omega_2^2 x_3 + \mu_2(1 - x_3^2)x_4 + \alpha(x_1 - x_3) + u(x_1, x_2, x_3, x_4) \tag{25}$$

where, $u(x_1, x_2, x_3, x_4)$ is the synchronizing signal. Define the synchronization error as,

$$e_1 = x_1 - x_3, e_2 = x_2 - x_4 \tag{26}$$

The synchronization error dynamic is:

$$\begin{aligned} \dot{e}_1 &= e_2 \\ \dot{e}_2 &= -(\omega_1^2 + \alpha)x_1 + (\omega_2^2 - \alpha_1^2)x_3 + \mu_1 e_2 \\ &\quad + (\mu_1 - \mu_2)x_4 - \mu_1 x_1^2 x_2 + \mu_2 x_3^2 x_4 - u \end{aligned} \tag{27}$$

The control signal u is obtained from feedback linearization as follow:

$$u = (\mu_1 - \mu_2)x_4 - \mu_1 x_1^2 x_2 + \mu_2 x_3^2 x_4 + k e_2 - (\omega_1^2 - \omega_2^2)x_3 \tag{28}$$

where, k is a scalar number and used for error dynamic stabilization. By rewriting the error dynamical equation in matrix form:

$$\begin{aligned} \dot{e} &= Ae \\ A &= \begin{bmatrix} 0 & 1 \\ -\omega_1^2 - \alpha & \mu_1 - k \end{bmatrix} \end{aligned} \tag{29}$$

The necessary and sufficient condition for stability is the satisfying the Hurwitz condition by A . The characteristic equation is:

$$\lambda^2 - (\mu_1 - k)\lambda + \omega_1^2 + \alpha = 0 \tag{30}$$

where, λ is the eigenvalue of matrix A . All eigen values are negative if:

$$\mu_1 - k < 0 \Rightarrow k > \mu_1 \tag{31}$$

The control signal in (28) is dependent on x_i , ($i = 1, 2, 3, 4$). There is access only to x_1 and x_3 . To overcome this problem, the observer (14) with defining g as (19) is considered by revising it as follows:

$$\begin{aligned} \dot{\hat{x}}_4 &= -\omega_2^2 \hat{x}_3 + \mu_2(1 - \hat{x}_3^2)\hat{x}_4 + \alpha(\hat{x}_1 - \hat{x}_3) \\ &\quad + g_2(x_1 - \hat{x}_1, x_3 - \hat{x}_3) + u(\hat{x}) \end{aligned} \tag{32}$$

By substituting $u(\hat{x})$ instead of $u(x)$ in (25) and defining error as (15), the error dynamical equation becomes similar to (20) that its stability was proven in Theorem 2. Therefore, the main system and observer trajectories converge together and $u(\hat{x})$ can synchronize two pacemakers.

Example 4 shown the observer and synchronizer performances for two unidirectional-coupled Van der Pol systems.

Simulation results

Example 1: Suppose 3 with $\omega_1 = 9, \mu = 10$ parameters. Figure 4 shows performance of the observer for $a = 10$. The initial conditions are $x_0 = [2 \ 10]^T$ and $\hat{x}_0 = [0 \ 0]^T$ for the system and observer, respectively.

Figure 4 shown that the error tends to zero rapidly. The convergence rate increases by increasing the observer gain a but the undershoot and overshoot

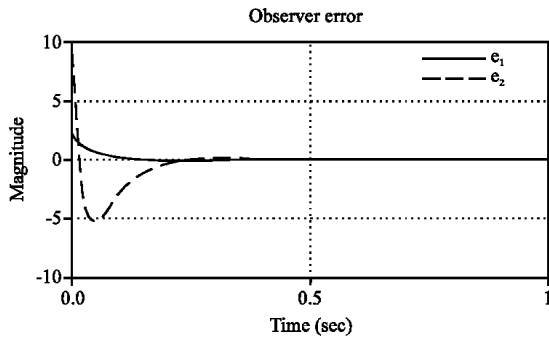


Fig. 4: Proposed observer performance for a unique van der Pol

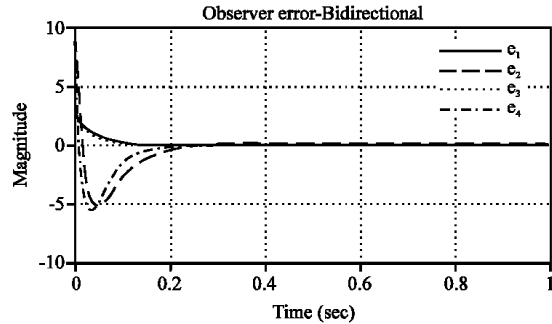


Fig. 6: Observer performance for two bidirectional coupled oscillators

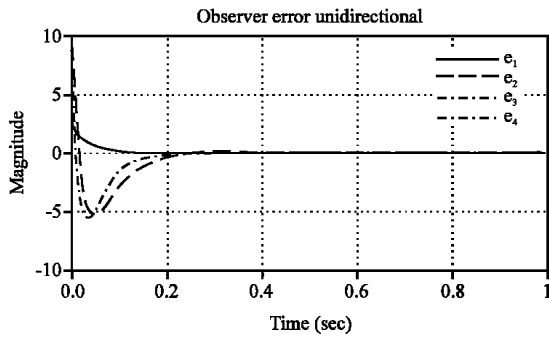


Fig. 5: Observer performance for two unidirectional coupled oscillators

increase relatively. In addition, in the presence of noise, the gain cannot be selected too large.

Example 2: Consider 13 with parameters $\omega_1 = 9, \mu_1 = 10, \omega_2 = 6, \mu_2 = 15, a = 80$. The observer system 14 performance with definition of 19 and $a_1 = a_2 = 10$ is shown in Fig. 5. The initial conditions are $x_0 = [2 \ 10 \ 2 \ 10]^T$ and $\hat{x}_0 = [0 \ 0 \ 0 \ 0]^T$.

It is observed from Fig. 5 that the error goes to zero before 0.2 s. by comparing error peaks of two Fig. 4 and 5, it is concluded that the error peaks of those are equal. The reason is that when (19) is used, the coupled system is divided in two isolated subsystems like (8). Therefore it is expected that their error peaks are equal.

Example 3: Consider (21) and (22) with parameters $a_1 = a_2 = 10, a_1 = 30, a_2 = 80, \omega_1 = 9, \mu_1 = 10$ and $\omega_2 = 6, \mu_2 = 15$. The initial conditions are selected as $x_0 = [2 \ 10 \ 2 \ 10]^T$ and $\hat{x}_0 = [0 \ 0 \ 0 \ 0]^T$. The observer error is shown in Fig. 6.

By increasing observer gain a_1 and a_2 , the speed of convergence increases while the undershoot/overshoot increases.

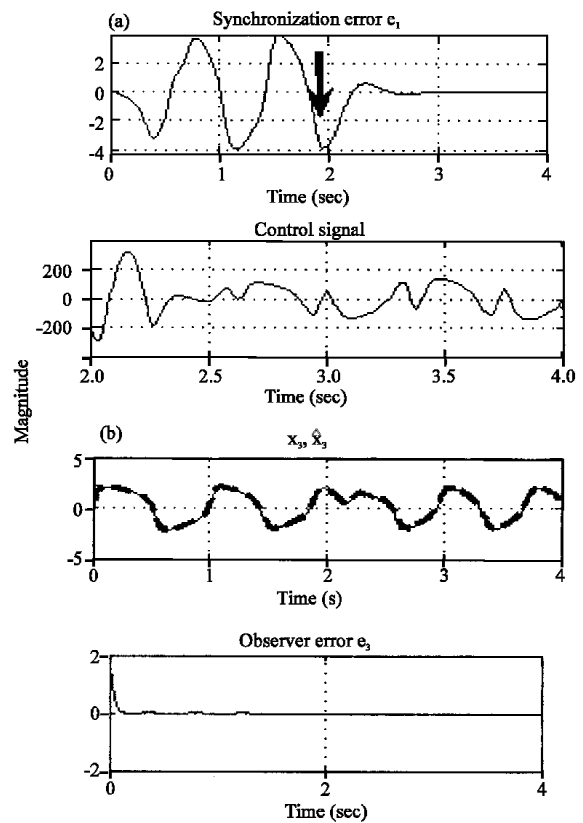


Fig. 7: Synchronization and Observer performances. (a) error between x_1 and x_3 state variables before and after synchronizer activation (synchronization error), (b) x_3 and \hat{x}_3 zstate variables and the error between them (the observer error)

Example 4: Assume parameters of two pacemakers as $\mu_1 = 10, \omega_1 = 9, \mu_1 = 15, \omega_2 = 6, \alpha = 20$, observer gains as $a_1 = a_2 = 10$ and synchronization gain as $k = \mu_1 + 10$. The parameters are considered such that the impulse generation rate of SA node is 60 min^{-1} and AV node

is 40 min^{-1} . The control signal is applied at $t = 2 \text{ sec}$. Figure 7a shows the synchronization error and the control signal and Fig. 7b illustrates the observer performance.

As the synchronization gain k increases, the convergence rate of error increases too but the amplitude of the control signal increases.

CONCLUSION

In this research, we introduced a robust observer for van der Pol system. We obtained the gain and phase margins for a range of parameters. The results show that the gain margin is always infinity and the phase margin is greater than 65° . The magnitudes of these criteria confirm the observer robustness. We used describing function method to prove the introduced observer stability. We extended the observer for two unidirectional and bidirectional coupled van der Pol oscillators. To prove the stability of new observer, we used the robustness properties. Since the coupled Van der Pol oscillators are used as cardiac pacemakers' model, for illustrating an application of the introduced observer, we designed a synchronization method for two unidirectional coupled pacemakers based on introduced observer. We used feedback linearization method to design synchronization system and demonstrated analytically that the synchronization error tends to zero exponentially.

APPENDIX

A: Consider the observer error dynamical equation for a unique van der Pol oscillator as:

$$\ddot{e} + \omega_1^2 e - \mu \dot{e} + \mu x_1^2 \dot{e} - \mu(\mu + a)e = 0 \tag{A1}$$

Assume the first harmonic frequencies of the variables of x and \hat{x} are not equal. Therefore the frequencies of x and e are not equal:

$$\begin{aligned} x(t) &= X \sin(\omega t), \hat{x}(t) = \hat{X} \sin(\omega' t), \omega \neq \omega', X \neq 0, \hat{X} \neq 0 \tag{A2} \\ e(t) &= X \sin(\omega t) - \hat{X} \sin(\omega' t) \end{aligned}$$

By substituting (A2) in (A1) and considering first harmonic:

$$\begin{aligned} &X[-\omega^2 + \omega_1^2 - \mu(\mu + a)] \sin(\omega t) - \hat{X}[-\omega'^2 + \omega_1^2 - \mu(\mu + a)] \sin(\omega' t) \\ &+ X\left(-\mu\omega + \frac{1}{4}\mu X^3\omega\right) \cos(\omega t) - \hat{X}\left(-\mu\omega' + \frac{1}{2}\mu X^3\omega'\right) \cos(\omega' t) = 0 \end{aligned} \tag{A3}$$

According to orthogonality of sinus and cosines functions and $\omega \neq \omega'$ assumption, we must have.

$$X = \hat{X} = 0 \tag{A4}$$

And this is contradiction. Suppose $\omega = \omega'$:

$$\begin{aligned} &\left[[-\omega^2 + \omega_1^2 - \mu(\mu + a)] \sin(\omega t) + \left(-\mu\omega + \frac{1}{4}\mu X^3\omega\right) \cos(\omega t)\right] \\ &\cdot (X - \hat{X}) = 0 \Rightarrow X = \hat{X} \end{aligned} \tag{A5}$$

It means that in steady state, in addition to frequency, the amplitude of x and \hat{x} is equal that is another confirmation to Theorem 1.

Notice: The (A5) cannot be achieved from (A3) directly. For that case, it should be done from the (A1)

B: We rewrite (21) and (22) as follow (Liao and Huang, 1999):

$$\begin{aligned} \dot{x} &= Ax + f(x, y) \\ y &= Cx \\ \dot{\hat{x}} &= A\hat{x} + f(\hat{x}, y) + L(y - C\hat{x}) \end{aligned} \tag{B1}$$

where, L is observer gain vector and:

$$\begin{aligned} x &= [x_1 \quad x_2 \quad x_3 \quad x_4]^T, \hat{x} = [\hat{x}_1 \quad \hat{x}_2 \quad \hat{x}_3 \quad \hat{x}_4]^T, y = [x_1 \quad x_3]^T \\ A &= \begin{bmatrix} 0 & 1 & 0 & 0 \\ -\omega_1^2 - \alpha_1 & \mu_1 & \alpha_1 & 0 \\ 0 & 0 & 0 & 1 \\ \alpha_2 & 0 & -\omega_2^2 - \alpha_2 & \mu_2 \end{bmatrix}, C = \begin{bmatrix} 1 & 0 & 0 & 0 \\ 0 & 0 & 1 & 0 \end{bmatrix} \\ f(x, y) &= [0 \quad -\mu_1 x_1^2 x_2 \quad 0 \quad -\mu_1 x_3^2 x_4]^T \\ f(\hat{x}, y) &= [0 \quad -\mu_1 \hat{x}_1^2 \hat{x}_2 \quad 0 \quad -\mu_1 \hat{x}_3^2 \hat{x}_4]^T \end{aligned} \tag{B2}$$

Since (A, C) is observable, there exist vector L such that (A-LC) is Hurwitz. According to (B1), the error dynamical equation is:

$$\dot{e} = \dot{x} - \dot{\hat{x}} = (A - LC)e + f(x, y) - f(\hat{x}, y) \tag{B3}$$

In addition, $f(\cdot, y)$ is globally Lipschitz, because:

$$\begin{aligned} &1 - f(0, y) = 0 \\ &2 - \|f(x, y) - f(\hat{x}, y)\| = \left\| \begin{bmatrix} 0 \\ -\mu_1 x_1^2 (x_2 - \hat{x}_2) \\ 0 \\ -\mu_2 x_3^2 (x_4 - \hat{x}_4) \end{bmatrix} \right\| \leq \gamma \left\| \begin{bmatrix} 0 \\ x_2 - \hat{x}_2 \\ 0 \\ x_4 - \hat{x}_4 \end{bmatrix} \right\| \leq \gamma \|x - \hat{x} \end{aligned} \tag{B4}$$

where $\gamma = \max(\mu_1 x_1^2, \mu_2 x_2^2)$, x_1 and x_2 are the van der Pol oscillator state variables. Since van der Pol oscillator state variables are bounded therefore γ exists.

Suppose $e(0) = x(0) - \hat{x}(0)$ as error initial condition. The solution of (B3) is:

$$e(t) = e^{(A-LC)t} e(0) + \int_0^t e^{(A-LC)(t-\tau)} [f(x(\tau), y(\tau)) - f(\hat{x}(\tau), y(\tau))] d\tau \quad (B5)$$

Since (A-LC) is Hurwitz, therefore there exist $\alpha > 0$, $m > 1$ such that:

$$\|e^{(A-LC)t}\| \leq m e^{-\alpha t} \quad \forall t > 0 \quad (B6)$$

And for $e(t)$:

$$\begin{aligned} \|e(t)\| &\leq m \|e(0)\| e^{-\alpha t} + m \int_0^t e^{-\alpha(t-\tau)} \|f(x(\tau), y(\tau)) - f(\hat{x}(\tau), y(\tau))\| d\tau \\ &\leq m \|e(0)\| e^{-\alpha t} + m \gamma e^{-\alpha t} \int_0^t e^{-\alpha(t-\tau)} \|e(\tau)\| d\tau \end{aligned} \quad (B7)$$

By multiplying (B7) to $e^{\alpha t}$ and using Bellman-Grownwall Lemma:

$$\|e(t)\| \leq m \|e(0)\| e^{-(\alpha-m\gamma)t} \quad (B8)$$

Therefore, if the condition $\alpha > m\gamma + \delta, \delta > 0$ holds, the error dynamical system is exponentially stable. By choosing a proper vector L, the condition holds for van der Pol oscillator.

REFERENCES

- Brando, D.D., M.G. Signorini and S. Cerutti, 1998. A model of two nonlinear coupled oscillators for the study of heartbeat dynamics. *Int. J. Bifurcation Chaos*, 8: 1975-1985.
- Fitzhugh, R., 1961. Impulses and physiological states in theoretical models of nerve membrane. *Biophys. J.*, 1: 445-466.
- Floret-Ponet, F. and F. Lamnabhi-Lagarrigue, 2001. Parametric identification methodology using sliding modes observer. *Int. J. Control*, 74: 1743-1753.
- Grudzinsky, K. and J. Zebrowski, 2004. Modeling cardiac pacemakers with relaxation oscillators. *Phys. A.*, 336: 153-162.
- Guyton, A.C. and J.E. Hall, 2005. *Medical Physiology*. 11th Edn., W.B. Saunders Co., Philadelphia PA-USA., ISBN: 0-7216-02401.
- Hua, C., X. Guan, X. Li and P. Shi, 2004. Adaptive observer-based control for a class of chaotic systems. *Chaos Solitons Fractals*, 22: 103-110.
- Julier, S.J. and J.K. Uhlmann, 1997. A new extension of the Kalman filter to nonlinear systems. *Int. Symp. Aerospace/Defense Sens., Simul. Controls*, pp: 1-12, http://www.cs.unc.edu/%7Eewelch/kalman/media/pd/f/Julier1997_SPIE_KF.pdf.
- Kalman, R.E., 1960. A new approach to linear filtering and prediction problems. *Trans. ASME. J. Basic Eng.*, 82: 35-45.
- Liao, T.L. and N.S. Huang, 1999. An observer-based approach for chaotic synchronization with application to secure communications. *IEEE. Trans. Circ. Sys. I: Fundamental Theory Appli.*, 46: 1144-1150.
- Nagumo, J., S. Arimoto and S. Yoshizawa, 1962. An active pulse transmission line simulating nerve axon. *Proc. Inst. Radio Eng.*, 50: 2061-2070.
- Pearson, J.D., 1962. Approximation method in optimal control. *J. Elect. Control*, 13: 453-465.
- Sato, S., S. Doi and T. Nomura, 1994. Bonhoffer-van der pol oscillator model of the Sino-Atrial node: A possible mechanism of heart rate regulation. *Methods Inform. Med.*, 33: 116-119.
- Slotine, J.E. and W. Li, 1991. *Applied Non-Linear Control*. 1st Edn., Prentice Hall, New Jersey, ISBN: 9780130408907.
- Van der Pol, B. and J. van der Mark, 1927. Frequency demultiplication. *Nature*, 120: 363-364.
- Zhang, C., X.X. Zhou, Y.J. Cao and Q.H. Wu, 1999. Disturbance auto-rejection control of TCSC. *Control Eng. Pract.*, 7: 195-199.